Finite element simulation of mechanical properties of graphene sheets

IOP Conf. Series: Materials Science and Engineering **206** (2017) 012057 doi:10.1088/1757-899X/206/1/012057

Finite element simulation of mechanical properties of graphene sheets

N Khandoker*, S Islam, Y S Hiung

Department of Mechanical Engineering, Curtin Malaysia, CDT 250, Miri 98009, Sarawak, Malaysia.

*E-mail: noman.khandoker@curtin.edu.my

Abstract. Graphene is the material for the twenty first century applications. In this paper, the elastic properties of monolayer and double layer Graphene sheets, typically less than 10nm in size are investigated through linear finite element simulations. The effect of aspect ratio, sizes and chirality of the Graphene sheet on the Young's modulus, Shear modulus and Poisson's ratio are studied. By using structural mechanics approach combining atomistic and equivalent continuum techniques, the Young's modulus, shear modulus and the Poisson ratio were found and they slightly increase with the aspect ratio but decrease with the size of the Graphene sheet. These simulated properties compliment the mechanical properties of Graphene found in literature.

1. Introduction

Graphene has been discovered for about ten years since 2004 and its area of research grew extremely fast that hundreds of laboratories all over the world deal with different aspects of graphene research nowadays, which is driven by its uniqueness of possessing remarkable properties such as high electrical and thermal conductivity [1]. In addition, graphene is also considered to be a promising material for spintronics and spin qubits which will allow for massive increase in future computational power [2].

Besides, graphene also gave birth to a new class of crystal such as fluro-graphene, boron nitride, [3] and molybdenum disulphide [4] that are also just one atom thick. Recently, graphene related two-dimensional crystals and its hybrid systems were found to be available in energy conversion and storage for future applications [5]. Furthermore, composite materials with graphene as reinforcements are also feasible and beneficial for many applications. For example, in case of corrosion prevention, graphene grown on carbon steel with Nickel catalysts, provide almost 7 times more corrosion resistance than that of the original steel [6]. Hence, it is important to understand the mechanical behavior of graphene sheets in facilitating a better characterization of the resulting nano-composites in its future applications of different industries.

Therefore, the objectives of this current study are to investigate the effect of sizes, chirality and aspect ratios of graphene on its mechanical properties such as Young's modulus, shear modulus and Poisson's ratio. Furthermore, the effects of Van der Waal's interactions in double layered graphene on its mechanical properties are also investigated.

2. Literature Review

Calculations for the elastic modulus of single layer graphene sheet can range from quantum mechanics calculations to molecular dynamic, atomistic simulations and continuum models. Molecular dynamics and ab initio methods are quite popular methods in determining the elastic properties of nano materials such as carbon nanotubes and graphene.

Molecular dynamics method has been used by Lu [7] to determine the Poisson's ratio and Young's modulus of carbon nanotube. In this model, the force constants were empirically determined by fitting to measured elastic constants and the phonon frequencies. This phonon spectrum of graphite and the Poisson's ratio are calculated by minimizing the strain energy with respect to both the radial compression and the axial extension with the wall thickness of 0.34 nm. The results showed an averaged Poisson ratio of 0.28 and Young's modulus of 0.974 TPa for the nanotubes of various sizes.

Hernandez et al. [8] did a similar construction for the single wall carbon nanotubes and some other composite nanotubes using a non-orthogonal tight binding model. The average Poisson's ratio and Young's modulus of different sizes of nanotubes were 0.262 and 1.24 TPa respectively. Meanwhile, the ab initio study of Gregory et. al used an implementation of the theory of Hartree–Fock 6-31G* level, and an ab-initio multiplicative integral approach for the calculations [9]. The results revealed that Young's Modulus of graphene is 1.11 TPa. Ricardo et al. also used ab initio method to investigate the structural, electronic and mechanical properties of zigzag graphene nano-ribbons in the presence of stress by applying density functional theory within the GGA-PBE (Generalized Gradient Approximation-Perdew–Burke–Ernzerhof) approximation [10]. The average Young's modulus generated was 0.96 TPa with the thickness of 0.335 nm and the Poisson's ratio found was 0.17.

A more recently used method is the structural mechanics method combining atomistic and continuum modelling techniques. In this modelling technique, the graphene structure are modelled at nano-scale with every detail concerning the position of atoms and the force field connecting them. However, the connections for each atom of the lattice molecular structure are replaced with a continuum medium of an specific element type representing the force field.

A. Sakhaee-Pour [11] adopted an atomistic simulation model comprised of structural beam which simulates the covalent forces of the carbon atoms using potential energy of bond bending, bond stretching, out of plane and dihedral torsional of bond. The model was considered for the shape of the graphene sheet and investigations were performed for various chirality.

3. Methodology

For this study, a structural mechanics method is adopted with atomistic and continuum techniques approach to investigate the elastic characteristics of defect-free single-layered and double layered graphene sheet. The atomistic model used finite beam elements to simulate the covalent bonds between the carbon atoms. The elasticity of the beam elements are characterized into the molecular and structural potential energies in term of stretching, bending, and torsional potential energies based on Odegard's methodology. [20]

From the work of Raji Heyrovska, it is described that a graphene hexagon which consists of 7 carbon atoms, has a carbon-carbon bond length of approximately 1.42 Å and the bond angle between the covalent bond is 1200 to each other [12]. Hence using this information, the graphene sheet structure can then be modelled with respect to the Cartesian coordinate system (x, y, z) as shown in figure 1 and figure 2. The modelling of the graphene is done by Visual Molecular Dynamic (VMD) software and the scale used in the model is in Angstrom or 0.1nm. The interatomic distance between

the adjacent carbon atoms which belong to the same plane is modelled as 1.418 Å and the interlayer spacing or the thickness of the graphene sheet is approximately equal to 0.34 nm.

Neglecting the van der Waal forces and the interatomic electrostatic interaction, the total molecular potential energy, UT can be considered as the following equation:

$$U_T = \sum U_r + \sum U_\theta + \sum U_\tau \quad (1)$$

where U_r is the bond stretching energy, U_θ is the angle bending energy and U_τ is the torsional potential energy which includes the out of plane and dihedral angle torsions. Each of these molecular potential energies is related to its respective degree of freedom by a force field constant known as stiffnesses and are independent to each other. The relationships with the stiffnesses are as shown in equations 2, 3, and 4 below:

$$U_r = \frac{1}{2}\, k_r\, (r - r_o)^2 = \frac{1}{2} k_r (\Delta r)^2 \quad (2)$$

$$U_\theta = \frac{1}{2} k_\theta (\theta - \theta_o)^2 = \frac{1}{2} k_\theta (\Delta\theta)^2 \quad (3)$$

$$U_\tau = \frac{1}{2} k_\emptyset (\emptyset - \emptyset_o)^2 = \frac{1}{2} k_\tau (\Delta\emptyset)^2 \quad (4)$$

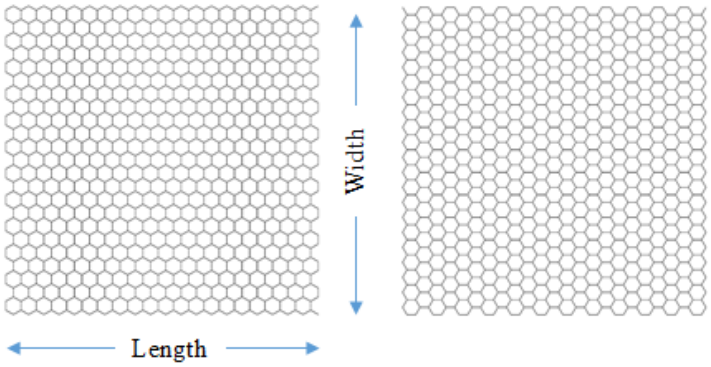

Figure 1. Armchair (left) and Zigzag (right) shapes of single layered graphene sheets

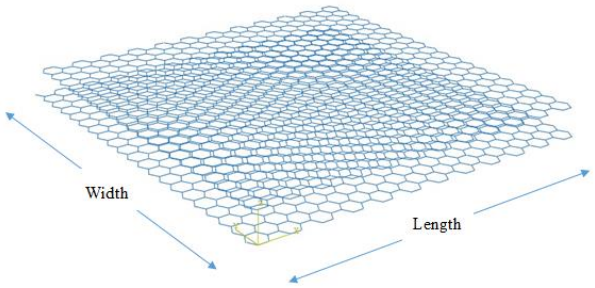

Figure 2. Armchair shape of double layered graphene sheet

where k_r, k_θ, and $k_\emptyset$ are the bond stretching, angle bending and torsional stiffnesses respectively and Δr, Δθ, and Δ∅ are the corresponding displacement in its respective degree of freedom. Based on structural mechanics, the potential energy for strain energy for a uniform beam is expressed as equation 5 below. The bending potential energy under a pure bending load is expressed as the equation 6 while the torsional potential energy for pure torsional load is expressed as equation 7:

$$U_A = \frac{1}{2}\int_0^L \frac{N^2}{EA}\, dl = \frac{1}{2}\frac{N^2 L}{EA} = \frac{1}{2}\frac{EA}{L}(\Delta L)^2 \quad (5)$$

$$U_M = \frac{1}{2}\int_0^L \frac{M}{EI}dl = \frac{2EI}{L}\alpha^2 = \frac{1}{2}\frac{EI}{L}(2\alpha)^2 \quad (6)$$

$$U_T = \frac{1}{2}\int_0^L \frac{T^2}{GJ}dl = \frac{1}{2}\frac{T^2L}{GJ} = \frac{1}{2}\frac{GJ}{L}(\Delta\beta)^2 \quad (7)$$

where A is the cross section of the beam, L is the beam length, ΔL is the displacement in length and E the Young modulus of the considered beam for equation 5. In equation 6, I and α represent the moment of inertia and rotational angle of the beam ends while in equation 7, $\Delta\beta$ is the relative bending angle, G represents the shear modulus, and J is the polar moment of inertia.

In order to simulate the molecular potential by structural means, the molecular potential energy are imposed into the structural potential energies by equating equations 2, 3 and 4 with 5, 6, and 7 respectively. This can be done since the potential energy terms in each system are independent to each other. By doing this, the stiffness of the equivalent structure beam can then be related in term of the force field constants as shown in equations 8 below:

$$\frac{EA}{L} = k_r \quad \frac{EI}{L} = k_\theta \quad \frac{GJ}{L} = k_\emptyset \quad (8)$$

The force field constant of graphene is taken from J. Medina based on the linear density approximation results as shown in table 1 below. [13] It is noted that with the stiffness related to the force field constant, the stiffness matrix can then be applied to the structural beam. However, in this study, that approach is not going to be followed. Instead, the approach will be the finite element analysis method where the characteristic of the beam is fulfilled by the beam elastic moduli and diameter.

$$A = \frac{\pi d^2}{4} \quad I = \frac{\pi d^4}{64} \quad J = \frac{\pi d^4}{32} \quad (9)$$

Hence, the Young's modulus, shear modulus and the beam diameter is calculated by substituting the relationships as shown in equations 9 to the beam characteristic relationship in terms of the force field. The derived equations for the beam elastic moduli and the corresponding diameter are as shown in equations 10 and the values are tabulated in Table 2.

$$d = 4\sqrt{\frac{k_\theta}{k_r}} \qquad E = \frac{k_r^2 L}{4\pi k_\theta} \qquad G = \frac{k_r^2 k_\emptyset L}{8\pi k_\theta^2} \quad (10)$$

Table 1. Values of the force field constants

Force field constant	Values
Bond stretching stiffness, $\boldsymbol{k_r}$	740 N/m
Bond bending stiffness $\boldsymbol{k_\theta}$	7.69 x10-19 Nm/ rad^2
Bond torsional stiffness $\boldsymbol{k_\emptyset}$	2.78 x10-19 Nm/ rad^2

Table 2. Values of beam characteristics

Beam Characteristics	Values
Beam's diameter, d	1.29x10-10 m
Beam's elastic modulus, E	8.05 x1012 N/m^2
Beam's shear modulus, G	1.45x1012 N/m^2

For double layered graphene sheet, the Van der Waal forces of interaction are modelled as truss beam structure with approximate non-linear characteristics. The non-linear relationship of the Van der Waal forces between the graphene sheets is usually modelled by using the Lennard-Jones 6-12 potential energy equation as shown below:

$$U_{vdw}(r) = 4\varepsilon_{vdw}\left[\left(\frac{\sigma_{vdw}}{r}\right)^{12} - \left(\frac{\sigma_{vdw}}{r}\right)^{6}\right] \quad (11)$$

where σ_{vdw} is the finite distance at which the inter-particle potential is zero (in case of graphene, σ is 0.34 nm), r is the distance between the particles, and ε_{vdw} is the depth of the potential well. For graphene and carbon nanotube, it is given by 3.8655×10^{-13} N nm from the work of Odegard et.al. [20]. In this study, the non-linear characteristic of the Van der Waal forces is compared to the structural strain energy of the truss element used in the model and the expression of the Young's modulus is obtained as has done by A. Parashar et.al. [14] The expression for the Young's modulus is as shown below:

$$E(r) = \frac{8R_{eq}\varepsilon_{vdw}}{A_t(r-R_{eq})^2}\left[\left(\frac{\sigma_{vdw}}{r}\right)^{12} - \left(\frac{\sigma_{vdw}}{r}\right)^{6}\right] \quad (12)$$

where R_{eq} is equilibrium distance for Van der Waals forces (0.3816nm), A_t is cross sectional area for a truss element (0.0907 nm2) and $E(r)$ is the estimated Young's modulus for the truss element [14]. For this simulation, the average interatomic distance of the double layered graphene is taken to be the value of r which is found to be 0.36378 nm. Hence, the value of the average Young's modulus for the truss element is evaluated $as\ 9.10 \times 10^{-9}$ N nm^{-2}. For simplicity of the simulation, this material property is defined for the all truss elements in the model.

In the model, each of the atoms in the upper layer is connected to either four of the atoms (type 1 interaction) or six of the atoms (type 2 interaction) in the lower layer via the truss elements. The Van der Waals interaction for type 1 and type 2 are as shown in Figure 3. The double layered graphene model with the truss elements as the Van der Waal forces is shown in Figure 4.

4. FEA Simulation

By having all the information required for the beam, the model can then be simulated. However, the structure of single layered graphene are 2-dimenisonal and hexagonal in shape which have many empty spaces in between the structure. This implies many difficulties in applying forces or boundary conditions on the graphene sheet to obtain the elastic moduli of the graphene.

Coupling constraints were used for the boundary conditions of this model. The boundary conditions applied to both ends of the graphene sheet were done by using kinematic coupling constraints with a control point at a reference point located at the middle of both ends of the graphene. This constraint was applied to make sure the boundary conditions are applied to every point of the edge as equivalence to a continuum structure.

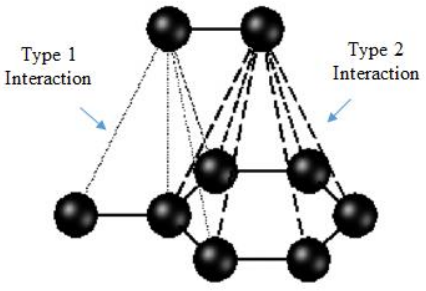

Figure 3. Truss Representing Van der Waals Forces

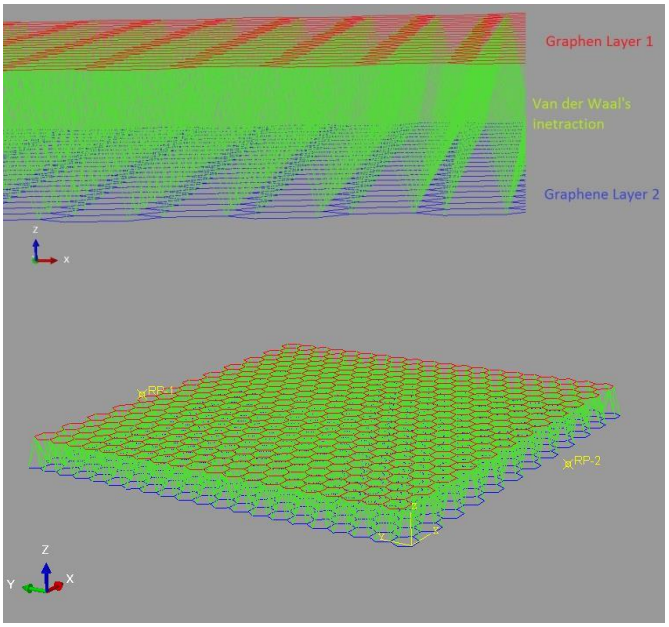

Figure 4. Double Layered Graphene Model

In order to understand the elastic behaviour of the graphene layer under tension, perpendicular forces needed to be applied to the free edge of the graphene sheet. However, instead of applying forces, displacement boundary conditions are set in this study. This can be done by applying Hooke's law which stated that the linear elastic displacement was directly proportional to the forces acted in the displacement direction as long as the elastic limit is not exceeded.

The boundary condition was set to be fixed in all degree of freedom at one end while the other end was subjected to a displacement of 10% of its width in the y-direction for tensile load or length in the x-direction for shear load.

In this study, the elastic properties of the graphene sheet were predicted to be dependent on the chirality. Therefore, zigzag and armchair shaped graphene sheet were modelled and investigated. The variables considered in this study were basically the size and shape. However, in this study, the length to width ratio of graphene sheet is also varied. The size considered includes square shaped graphene with length of 3nm, 5nm, 7 nm and 10nm. For length to width ratio analysis, five lengths to width ratio of approximate 0.33, 0.5, 2 and 3 are done in this simulation. A double layer was also done to analyse the effect of number of layer to the Young's modulus.

The model can be equalled to a continuum model, it can then be said that the normal stress, σ of the continuum sheet can be found using the classic stress definition given by the ratio of force to cross sectional area as Equation 13 below:

$$\sigma = \frac{f_n}{bt} \tag{13}$$

where f_n is the magnitude of the tensile forces computed from simulation, b is the graphene length and t is the thickness of the graphene. Hence, the Young's modulus of the graphene sheet can be computed by using the relationship of normal stress and strain as the following equation 14:

$$E = \frac{\sigma}{\varepsilon} = \frac{f_n w}{bt\Delta w} \tag{14}$$

where ε represents the tensile strain that is defined as the ratio of elongation, Δw to the graphene sheet initial width, w. On the other hand, the shear stress of the continuum sheet can also be found using the similar manner as the normal stress shown equation 11. However, the forces required are the

tangential forces to the free edge of the graphene sheet. The expression for shear stress is as shown in equation 15 below:

$$\tau = \frac{f_s}{bt} \tag{15}$$

where, f_s is now the magnitude of the shear forces computed from simulation. Therefore, the shear modulus, G of the graphene sheet is also able to be computed by using the following equation 16 where γ is the shear strain of the graphene sheet under shear stress:

$$G = \frac{\tau}{\gamma} = \frac{f_s}{\gamma bt} \tag{16}$$

The shear strain of the graphene sheet can be computed using the boundary conditions set for the shear stress condition as shown in equation 17 below, where Δb is the displacement in the length.

$$\gamma = \frac{\Delta b}{w} \tag{17}$$

By obtaining the Young's modulus, shear modulus and the results from the simulation, the Poisson ratio can finally be calculated for the zigzag and armchair graphene sheet. The Poisson ratio, based on Hooke's law on elastic properties can be computer via the Equation 18 as shown below:

$$v = \frac{E}{2G} - 1 \tag{18}$$

5. Results and Discussion

5.1. Size and Shape Analysis

In the first parametric study, a single layer armchair graphene was studied by increasing the size (length and width) of the graphene. Then, a single layer zigzag graphene was studied by using the same size as the studied armchair graphene.

From the simulations, the reaction forces obtained are plotted against the length of the graphene as in Figure 5. It shows that, the reaction force has a linear relationship to the length of the graphene. These results are actually well predicted since the loading displacements are fixed 10% of its original height. Therefore, since the force is directly proportional to the number of nodes, the bigger the size (length) of the graphene, the higher the number of nodes, hence, the higher the reaction forces.

However, the more obvious result from the reaction force obtained is that the armchair graphene has a higher reaction force when compared to zigzag graphene with the same size. This may because the direction of the load applied to all the armchair graphene's covalent bonds (beams) are tilted at an angle of 600 while in the zigzag graphene, the direction of the load applied is parallel to some of the covalent bonds. With the tilted covalent bonds, more forces are required to increase the distance between them compared to a straight covalent bond as bending of the bonds are involved too in the tilted condition. Therefore, higher force was observed in the armchair graphene.

The reaction forces obtained from the simulation were utilized to calculate the Young's Modulus and the Shear Modulus and these results are plotted with respect to their corresponding sizes in Figure 6 and 7. From Figure 6, it is clear that the Young modulus are in the range of 0.8TPa to 0.95TPa. [16], [17], [18] and [21]. These results are slightly lower than those obtained from the literature which reported to be around be around 1.0 TPa. However, since different force constants are used, these results are deemed acceptable. For the shear modulus, the calculated results are in the same order as those reported in literature, approximate 0.25TPa to 0.45TPa. Although slightly lower, but low shear modulus also has been reported as in [11] and [15].

Besides that, it is also obvious that the Young's modulus of armchair graphene is greater than that of zigzag graphene when comparing the same size. This is as discussed in the reaction force before, since the armchair graphene required a higher force to have a 10% strain, the Young's modulus will certainly be higher. In other word, the armchair graphene will require more stress or force per unit area for every 1% strain increment. Moreover, these findings are consistent with the published literature [19].

Based on the graph in Figure 6, it can also be noted that the Young's modulus for both armchair and zigzag decreases with size due to hexagonal structure of graphene sheet. As the size of graphene sheet increases, the effect of side shrinkage becomes more obvious. The shrinkage of side of the graphene sheet may reduce the force required to increase the defection. Hence, the Young's modulus decreases as the size of graphene increases. However, it is reported in [19] that these phenomena seem to disappear as the length and width of graphene increases. Hence, further study and research on this matter is still necessary.

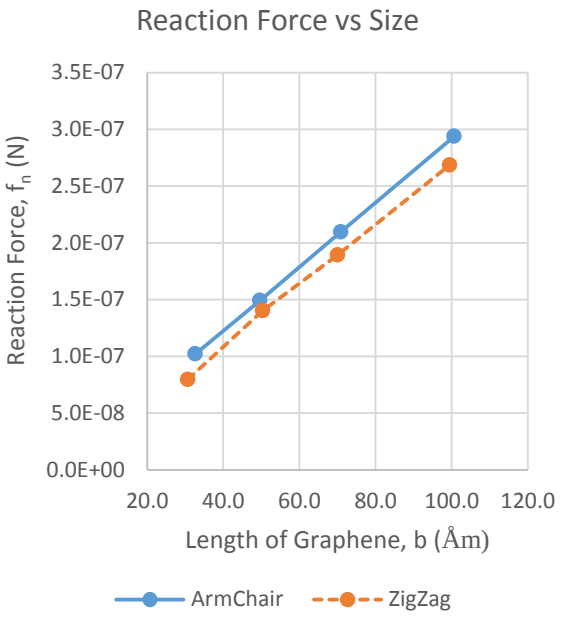

Figure 5. Graph of Reaction Force vs Size of Armchair and Zigzag Graphene

From the Young's modulus and shear modulus, the Poisson's ratio is then calculated as mentioned earlier. The calculated Poisson's ratio is then plotted against the size as shown in Figure 8. Based on the graph, the Poisson's ratio seems to be constant at around 0.8 for armchair graphene and 0.7 for zigzag graphene. The deviation of the constant Poisson ratio for the 3x3 nm graphene sheet may due to the aspect ratio slightly deviated from 1 to 1 ratio.

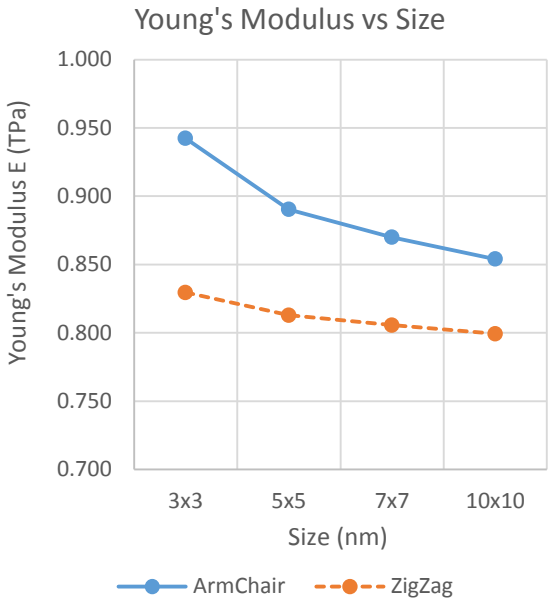

Figure 6. Graph of Young's Modulus vs Size of Armchair and Zigzag Graphene

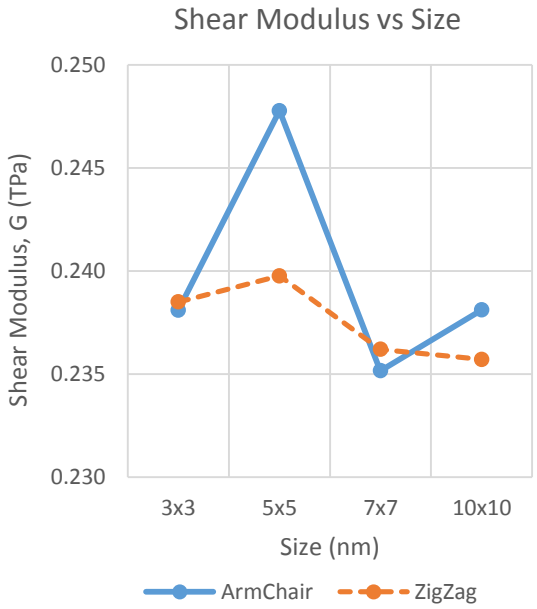

Figure 7. Graph of Shear Modulus vs Size of Armchair and Zigzag Graphene

5.2. Aspect Ratio and Shape Analysis:

In the second parametric study, a single layered armchair and zigzag graphene were studied by increasing the value of aspect ratio (length to width ratio) of the graphene. Similar to the study for effect of size, the reactions forces are obtained and the graph of reaction forces against aspect ratio for both armchair and zigzag graphene are plotted as shown in Figure 9 below. The graph plotted does not

show any significant relation between the force and the aspect ratio of the graphene. Instead, the reaction forces vary according to the length of the graphene as mentioned in previous section. Since the graphene with the aspect ratio 2 has the largest length value, thus it has a highest reaction forces. Meanwhile, the graphene with the aspect ratio of 0.33 has the lowest length value, hence it shows the lowest reaction force.

Based on the reaction force obtained, the Young's Modulus and the Shear Modulus are calculated for the corresponding graphene aspect ratio. The results are then plotted against the aspect ratio as shown in Figure 10 and 11 below. From Figure 10, it can be noted the Young's modulus seems to increase with the aspect ratio of the graphene and this is observed for both armchair and zigzag graphene. The gradient of the graph for armchair and zigzag are found to be almost similar to each other at approximate 0.06TPa for every 1 increment of the aspect ratio. This indicated that the Young's modulus of a single layer graphene sheet is also dependent on the aspect ratio. Besides, it is also worth to mention that the Young's modulus for armchair is higher when compared to zigzag graphene. This indicated that the results obtained for this analysis matches well with the previous section.

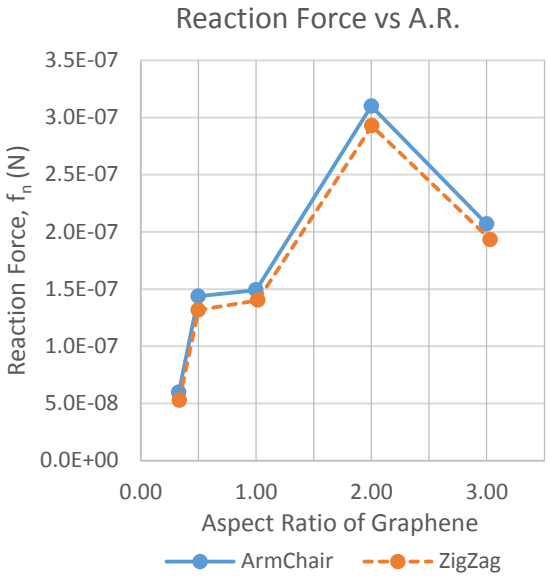

Figure 8. Graph of Reaction Force vs Aspect Ratio of Armchair and Zigzag Graphene

On the other hand, the effect of the aspect ratio to the Poisson ratio is remarkable. Similarly, to the previous section, using the Young's modulus and the shear modulus obtained, the Poisson's ratio are calculated for both armchair and zigzag and the results are plotted against the aspect ratio as shown in Figure 12. From Figure 12, the Poisson's ratio also increased with the aspect ratio, however, the gradient of the graph for the armchair graphene sheet is lower than that of the zigzag graphene. This shows that the Poisson's ratio of a single layer graphene sheet is also dependant on the aspect ratio with zigzag graphene having a higher effect. From the graph, it is also noticed that the line intersection for the armchair and zigzag graphene is at the aspect ratio value of 3. Hence, it is believed that as the aspect ratio greater than 3, the zigzag graphene would have a higher Poisson's ratio than armchair graphene.

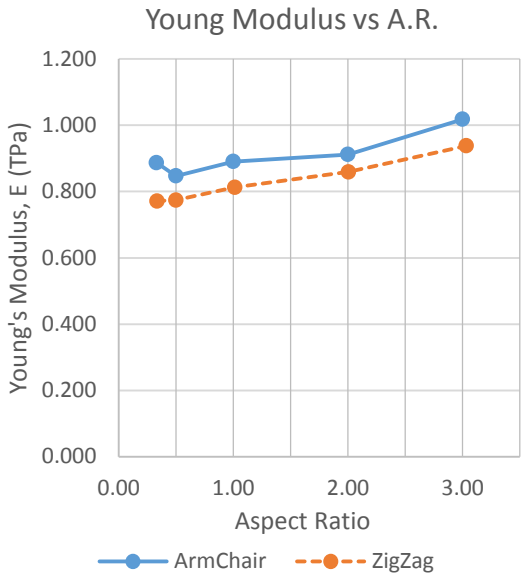

Figure 9. Graph of Young's Modulus vs Aspect Ratio of Armchair and Zigzag Graphene

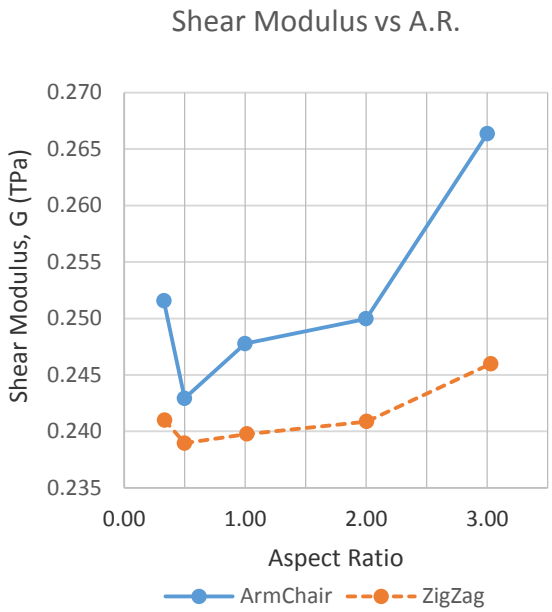

Figure 10. Graph of Shear Modulus vs Aspect Ratio of Armchair and Zigzag Graphene

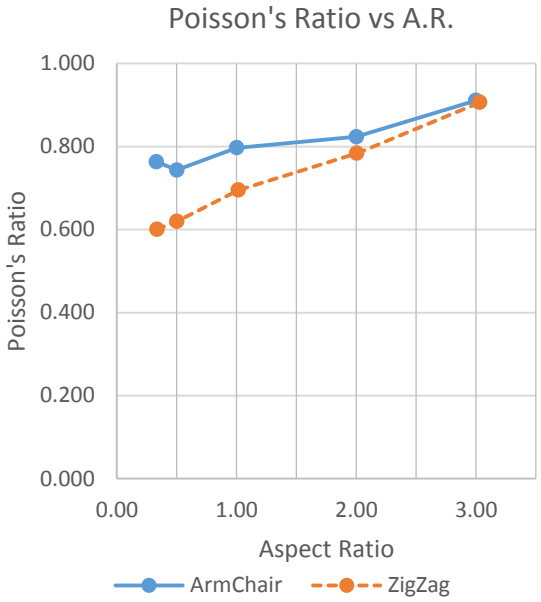

Figure 11. Graph of Poisson's Ratio vs Aspect Ratio of Armchair and Zigzag Graphene

5.3. Analysis of Double Layer Graphene Sheet:

A double layered graphene is also analysed in this study to determine any differences in the Young's modulus and Poisson ratio between a double layered and a single layered graphene sheet(s). For this parametric study, a 5x5 armchair double layered graphene sheets are modelled and simulated using the same procedure as the single layered graphene. The results obtained are compared with a single layered graphene with the same size, chirality and aspect ratio. The exact dimension of the double layered graphene and the results from simulation is as shown in Table 3.

Table 3. Comparison of single layered and double layered graphene properties

Parameter	Single Layered	Double Layered
Length (nm)	4.9630	5.0339
Width (nm)	5.0349	5.0349
Thickness (nm)	0.34	0.68
Reaction Forces (N)	1.492e-7	3.03e-7
Young's Modulus (TPa)	0.890	0.891
Shear Modulus (TPa)	0.248	0.238
Poisson's Ratio	0.794	0.872

From the table above, it can be seen that the Young's modulus for both single and double layered graphene are very similar to each other. This indicates that the Young's moduli of the graphene are independent to the number of layer. However, the Poisson's ratio of the double layered graphene is slightly higher than the single layered graphene. Hence, the Poisson's ratio might also dependant on the number of layer of the graphene sheet.

5.4. Comparison with Experimental Result:

Lastly it is of utter importance that the simulation results are compared with experimental results. Hence, the simulation results obtained in this study are compared with the available experimental results in the literature. Elastic properties of Graphene obtained from direct measurement experiments are preferred for this comparison. These comparisons are presented in Table – 4 below. It can be seen that the simulation results obtained in this study are in good agreement with the experimental results.

Table 4. Comparison of experimental and simulation results

Source	Approach	Sample	Young's Modulus (TPa)
Lee et. al [22]	Experimental (AFM)	Mono-layer graphene	1.0
Politano et. al [23]	Experimental (Phonon dispersion)	Macroscopic graphene sample	1.0
Current study	Simulation	Single layer graphene	0.890
Current study	Simulation	Double layer graphene	0.891

6. Conclusions

In conclusion, finite element simulations using atomistic modelling technique and continuum technique has been conducted on single layered and double layered graphene with a range of sizes and aspect ratios to determine the effect of size and aspect ratio to the Young's modulus, shear modulus and Poisson's ratio. In order to model the nanostructure, the mechanical properties of the carbon-carbon bonds were characterized as a circular beam element in which its elastic constants were properly defined. These elastic properties are determined by equating the potential energies of the molecular structure based on linear Hooke's law to the structural potential energy of the beam element.

In order to prove the validity of the model, the Young's modulus, shear modulus and Poisson's ratio found in this simulation were compared to the result found in literature and it matches well. Based on the simulation, the effect of size and aspect ratio on the Young's modulus and the Poisson ratio were identified. It is found that the Young's modulus increases slightly with the aspect ratio but decreases with the size while the Poisson's ratio also increases slightly with the aspect ratio but constant with size. The numbers of graphene layers affect the Poisson's ratio value but Young's modulus and shear modulus of this material remain unchanged within investigated parameters. These results are consistent with the current literature.

References

[1] Bolotin K I, Sikes K J, Jianga Z, Klimac M, Fudenberg G, Hone J, Kim P, and Stormer H L 2008 *Solid State Comm.* **146**(9-10) 351-355
[2] Novoselov K S, Blake P, and Katsnelson M I 2008, *Encyclo. of Mat.: Sci. and Techno. (Second Ed.)*, pages: 1-6
[3] Liu L, Park J W, David A Siegel, McCarty K F, Clark K W, Deng W, Basile L, Idrobo J C, Li A P, Gu G2014, *Sci.* **343**(6167) 163-167
[4] Najmaei S, Liu Z, Zhou W, Zou X L, Shi G, Lei S D, Yakobson B I, Idrobo J C, Ajayan P M, and Lou J. 2013, *Nature mat.* **12** (8) 754-759
[5] Bonaccorso F, Colombo L, Yu G H, Stoller M, Tozzini V, Ferrari A C, Ruoff R S, Pellegrini V. 2015, *Sci*. **347**(6217)
[6] Ye X H, Lin Z, Zhang H J, Zhu H W, Liu Z, and Zhong M L 2015, *Carbon* **94** 326-334

[7] Lu J P 1997, *Phy Rev. Lett.* **79(7)** 1297-1300
[8] Hernández E, Goze C, Bernier P, and Rubio A. 1998, *Phy Rev. Lett.* **80**(20) 4502-4505
[9] Van Lier G, Van Alsenoy C, Van Doren V, and Geerlings P 2000, *Chem. Phy. Lett.* **326**(1-2) 181-185
[10] Faccio R, Denis P A, Pardo H, Goyenola C, and Mombru A W. 2009 *J. of Phy.: Condensed Matter* **21**(28) 1-7
[11] Sakhaee-Pour A 2009, *Solid State Comm.* **149**(1-2) 91-95
[12] Heyrovska R, 2008, *arXiv:0804.4086v1.*
[13] Medina J, Avilés F & Tapia A. 2015, *Molecular Phy.* **113**(11) 1297–1305
[14] Parashar A, Mertiny P 2013, *Solid State Comm.* **173** (2013) 56–60
[15] Scarpa F, Adhikari S, and Srikantha Phani A 2009, *Nanotechno.* **20**(6) 1-11
[16] Georgantzinos S K, Giannopoulos G I, Katsareas D E, Kakavas P A, and Anifantis N K 2011 *Comp.Mat. Sci.***50** (7) 2057–2062
[17] Giannopoulos G I, Liosatos I A, and Moukanidis A K 2011, *Phy. E* **44** (1) 124–134
[18] Shokrieh M M, and Rafiee R 2010, *Mat. and Design* **31**(2) 790-795
[19] Georgantzinos S K, Giannopoulos G I, and Anifantis N K 2010, *Mat. and Design* **31**(10) 4646–4654
[20] Odegarda G M, Gatesb T S, Nicholsonc L M, and Wised K E 2002, *Composites Sci. and Techno.* **62**(14) 1869-1880
[21] Alzebdeh K. 2012, *Int. J. of Mech. and Mat. in Design* **8**(3) 269-278
[22] Lee C G, Wei X D, Kysar J W and Hone J, 2008, *Sci.* **321**(5887) 385-388
[23] Politano A, Marino A R, Campi D, Farı´as D, Miranda R, Chiarello G 2012 *Carbon* **50** 4903–4910